Heat transfer coefficient measurements on curved surfaces

MARCIN KUROWSKI*

Institute of Fluid Flow Machinery, Polish Academy of Sciences, Fiszera 14, 80-231 Gdansk, Poland

Abstract This paper presents the results of experimental research on heat transfer distribution under the impinging jets at high jet velocity on curved surfaces. The air jets flow out from the common pipe and impinge on a surface which is cooled by them, in this way all together create a model of external cooling system of low pressure gas turbine casing. Preliminary measurement results from the flat plate case were compared with the results from the curved surface case. Surface modification presented in this paper relied on geometry change of flat surface to the form of a 'bump'. The special system of pivoted mirrors was implemented during the measurements to capture the heat exchange on curved surfaces of the bump. The higher values of mean heat transfer coefficient were observed for all flow cases with a bump in relation to the reference flow case with a flat plate.

Keywords: Heat transfer coefficient; Measurements methodology; Gas turbine; Cooling

Introduction

Heat transfer is a critical issue in the development of aircraft engines. The external cooling systems of low pressure blades in modern aero engines are very complex and essentially rely on a series of circumferential feeding pipes. In such systems, impinging jets are directed towards the external turbine casing with the final aim of keeping the clearance between blade tip and casing as constant as possible under different engine operating conditions. A typical method for controlling those clearances is to actively control the

engine case temperature and then the static parts radial displacement dur-ing the different flight conditions.

Impinging air jets is a commonly used technique to cool advanced turbines elements, as it improves convection, thus enhancing the local heat transfer. Impinging is a complex phenomenon depending on many parameters, namely: Reynolds number, flow velocity, nozzle-to-plate distance, and radial position from the stagnation point. Therefore, many experimental studies have been carried out to evaluate the heat transfer characteristics on the surface under impinging jets. Several literature reviews on the heat transfer [1,2] and impingement heat transfer were published in the previous century and they underline the main results of studies concerning the topic of interest [3–6]. The effect of the parameters influencing the flow field and heat transfer characteristics of slot jet impingement have been investigated in the experimental and computational fields [7–9]. These studies on impingement heat transfer take into account the influence of the Reynolds number, where the jet velocity was rather low. They usually do not take into consideration the flow velocity effect. In fact, such approach brings in large that jet diameters at the Reynolds number similarity conservation are relatively high compared to those effectively used in a turbojet engine casing cooling system. As the Mach number can reach nowadays values as high as 0.4–0.5 and higher in modern turbojet turbines, this approach seems to be insufficient. Experimental studies which deal with this subject have been performed in [10]. It is found that additional phenomena start to play an important role in the heat transfer when the high velocity jet impinges the plate, *i.e.* only a portion of the total temperature is recovered by the test plate.

The effect of a row of impinging jets on plane surface on the local and average heat transfer coefficients has been investigated experimentally in [11]. Due to the collision of the spreading flows from nearby jets, the change of local heat transfer coefficient between the neighbouring jets has been re-ported. The maximum heat transfer coefficient at the stagnation point and its dependency on the jet to plate distance has been found. For different noz-zle to plate distances, Reynolds numbers and temperature differences used to determine the heat transfer coefficient, the recovery factor, the effective-ness and the heat transfer coefficient have been investigated. Kercher and Tabakoff [12] have shown in the experiment that the heat transfer is domi-nated by the hole diameter, Reynolds number and spacing-to-hole diameter ratio. Florschuetz *et al.* [13] presented correlations for both inline and stag-gered hole patterns including effects of geometric parameters: streamwise

hole spacing, spanwise hole spacing and channel height, normalized by the hole diameter.

The physical mechanisms influencing heat transfer coefficients as a result of flow distribution and geometric parameters are also discussed. Behbahani and Goldstein [14] presented experimentally the influence of jet-to-impingement plate and jet-to-jet spacing on the Nusselt number for dif-ferent Reynolds numbers. Goodro *et al.* [15] presented the experimental results of independent Mach number effects (as the Reynolds number is held constant) for an array of impinging jets. The discharge coefficients, local and spatially averaged Nusselt numbers, and local and spatially av-eraged recovery factors are discussed. Andreini *et al.* [16] evaluated both the heat transfer coefficient and the adiabatic thermal effectiveness charac-teristics of an engine-like ACC (active clearance control) system, and the effects of the undercowl flow on the impingement jets. Authors show an in-crease of heat transfer coefficient (HTC) when increasing the ACC pressure ratio, namely increasing the stagnation pressure by a factor of 1.15 they received an augmentation about 20% of HTC/HTCmax (where HTCmax is the maximum value of measured HTC coefficient) in the stagnation area of the jets. Ryfa *et al.* [17] investigated the reconstruction of the spatial dis-tribution of the HTC where the jet impingement heat exchange has been pursued by a hot air coming from the set of nozzles. The experiment was conducted to present the influence of selected geometric and flow parame-ters on the reconstructed heat exchange intensity. The results indicate an increase of the HTC with an increase in the Reynolds number. Authors have successfully reconstructed the HTC for the entire spectrum of tested parameters.

Very comprehensive review on the experimental and computational in-vestigations on the flow and thermal characteristics of jet impingement has been presented recently by Shukla and Dewan [18]. Measurements of the HTC on curved surfaces presented in this paper were followed by the ‘flat surface’ case [19]. Preliminary measurements of the heat transfer distribu-tion between the impinging orthogonally high velocity jets from long round pipe and flat plate lead to the better understanding of the heat exchange process and was the introduction for the measurements with curved sur-faces, which aimed to enhance the heat transfer on the low pressure turbine casing.

Measuring the heat transfer on a curved surface is quite a challenge, as it requires keeping the heating foil tightly adjacent to the wall at the measurement place. Ensuring good adherence of the heating foil is addi-

tionally hindered by the occurrence of a temperature gradient on the tested surface. Measurement of temperature distribution on the surface was performed by the use of liquid crystals in the steady state conditions of the system. Measurement of HTC is a difficult issue because it requires determination of heat flux reaching the tested surface with a good accuracy. In order to obtain this value on a curved surface, an appropriate approach to such measurement is required. The way, method of heat transfer coefficient measurement on a curved surface and linked with this challenges are presented in this paper. Finally the positive effect of a curved surface under impinging jets on heat transfer is presented.

2 Experimental setup

A view of the measurement test stand is shown in Fig. 1. This test sec-tion is a model of the turbine cooling casing system. Downstream of the inlet a pipe with a row of 26 jets is located. The jets outlet is connected to the vacuum tanks throughout the control valve. The test stand, apart from outlet pressure control, has a possibility to control independently the inlet pressure. A camera for temperature measurement of the test wall was located beneath the test section. Measurements were carried out for the arrangement of twenty six in-line jets with orifice diameter of d = 0.9 mm and the distance between jets about 6d. The outlet pressure correspond

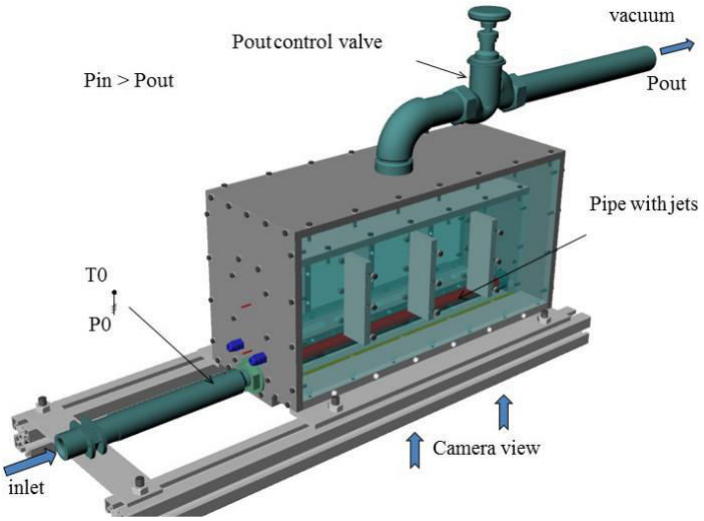

Figure 1: View of the test stand.

to aircraft cruise condition. Reynolds number (Re) based on the jet orifice exit conditions (jet orifice diameter has been taken as the characteristic length) was varied between 2500 and 4000. The flow velocity in the jets was particularly very high, changing from the Mach number Ma = 0.56 to 0.77. To investigate the heat transfer, liquid crystal (LC) sheet for temper-ature distribution measurements was placed on the surface under the jets, on the bottom wall of the test section. Measurements carried out on the curved surface let to maintain similarity with the complex geometry inside the external cooling system of the low pressure gas turbine casing.

The flow path through the test section is presented in Fig. 1. The ambi-ent air enters through the air filter, inlet control valve and mass flowmeter to inlet pipe where stagnation parameters of inlet gas are measured. The mass flow rate in the test section is controlled during the measurements by the precise needle control valve. Afterwards the air flows into the pipe with jets. The jets exit opens to a chamber of low pressure controlled by the P_{out} control valve. To investigate heat transfer the liquid crystal sheet for temperature distribution measurements was placed on the surface un-der the jets, on the bottom wall of the test section. All the heat transfer measurements were made on the bottom plate of the stand. It is fabricated of 15 mm thick transparent polymethyl methacrylate (PMMA). The im-pinging flow originates from the jets in the pipe above the plate, as it is shown schematically in Fig. 2 for two cases, ‘flat plate’ and ‘curved plate’ case. The only difference between the two above mentioned measurement cases is in the method of picture acquisition and post-processing of the data (described in the following section of the paper). The plate is covered with a 25 m thick heater foil (Inconel 625) on which a layer of self-adhesive LC foil is placed as shown in Fig. 2. The LC is sensitive to temperature between 30°C and 50°C.

The camera is a 3CCD JAY camera capable of taking 30 fps films with 24 bit colour depth (8 bits for each of the RGB components). The camera observes the LC foil through the transparent PMMA wall. On the other side, the LCs is covered with the heater foil (Fig. 2). The heater foil is powered by power supply system capable of controlling and supplying the necessary amount of power.

Summarizing, the following measurements were carried out during the tests:

- inlet flow stagnation parameters (temperature and pressure),
- temperature of the lower, outer surface of the measurement plate,

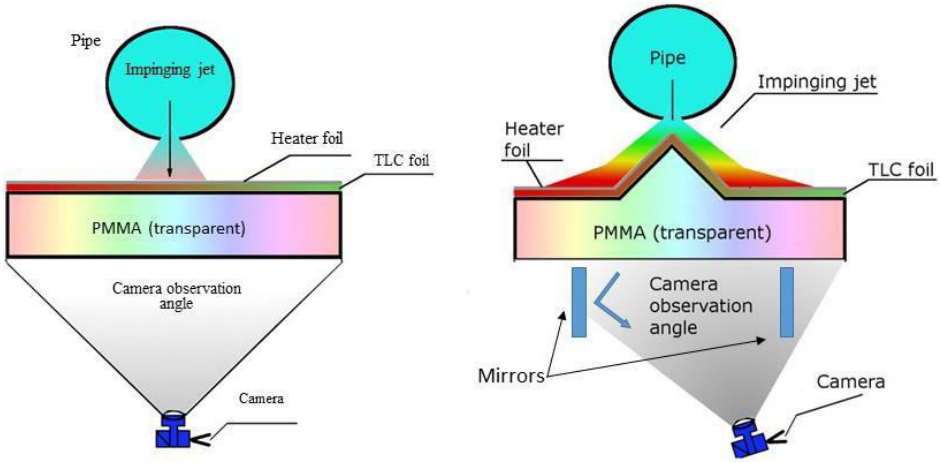

Figure 2: Measurement plate cross section schematic, left – flat plate case, right – curved plate case.

- temperature of the heater foil,
- temperature distribution on the test wall,
- heating power of the foil,
- pressures along the flow path,
- mass flow.

Figure 3 presents the air suction system introduced to remove the air to ensure the adjoining of LC covered foil and surface with a bump. The system consists of two ducts along the foil (1 mm width, 1 mm depth) and sets of holes (1 mm diameter) on the foil sides connected to the vacuum

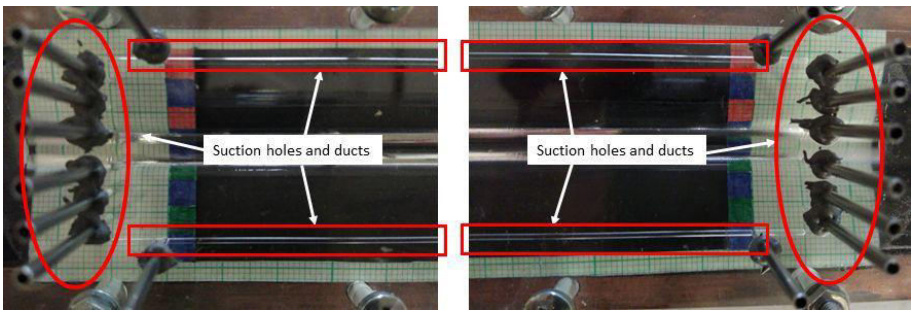

Figure 3: The air suction system – camera view, left and right side of the plate.

pumps. A lower pressure level in the suction system in relation to the test section has been kept by the vacuum pumps operating continuously during the measurement campaign.

3 Definition of area of interest

Due to the shape of the bump its region is not clearly visible in the picture taken by camera positioned perpendicularly to the plate (like in the setup depicted in Fig. 2 left). Therefore, three photographs are taken for each measurement case. One is like in the setup depicted in in Fig. 2 left and the frame from the central view for the bump case is presented in Fig. 4. The second picture is taken with the use of adequate place mirror in configuration not perpendicular to the plate (Fig. 2 right). The third picture is taken analogically, but with the camera tilted in the opposite direction. Such setup allows to get a clear photograph of one of the slope of the bump. An image obtained from the tilted position is depicted in Fig. 5.

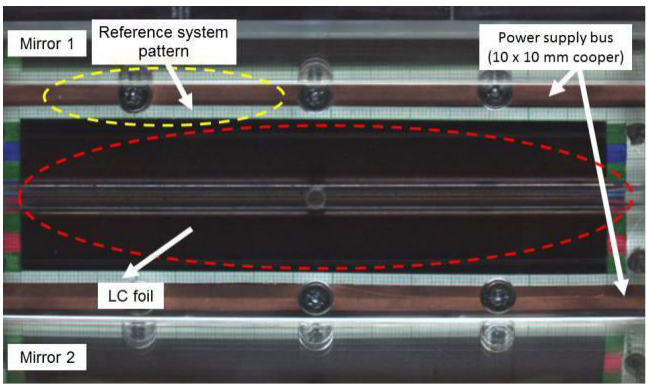

Figure 4: Actual frame taken by the camera in perpendicular position.

Due to the proportion of the measurement plate, the frame covers more than the region of the heater foil which is of the interest area. It was decided that the HTC distribution will be investigated in a region 10 mm longer than the length of the jets row (26 jets, spaced 5 mm in the pipe) and expanding 15 mm across from the jets centre line on the plate, as depicted in Fig. 6. The dashed lines indicate 26 jets, solid lines mark the centre of the jets row and region expanding 15 mm form the jets. The 15 mm distance was chosen as it is enough to embrace the region of significant activity of the impinging jet and still sufficiently distant from the power supply buses,

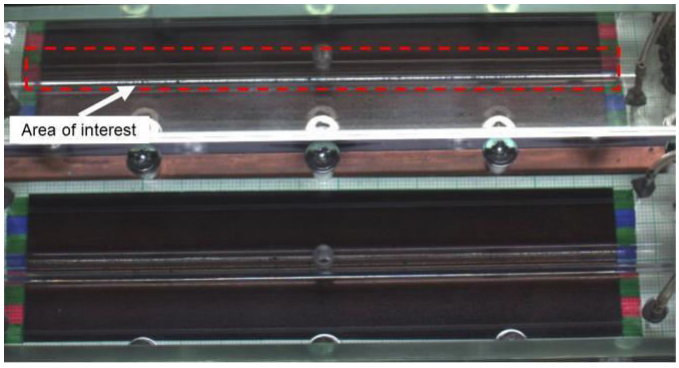

Figure 5: Actual frame taken by the camera in not a perpendicular (tilted) position.

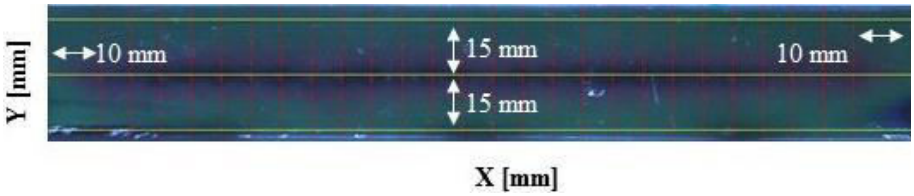

Figure 6: Definition of the interest region.

whose influence we neglect. The axial distance from extreme jets has been selected as twice the distance between the jets, which yields 10 mm.

To investigate the stability of the measurement method and equipment, all the test cases have been measured ten times. The time needed to obtain steady state conditions and then execute the measurement of heat transfer for one flow case was 7–8 hour, so it lasted one working day. Together with very detailed calibration, these measurements were very time consuming to be carried out. For all the measurements the distance between the jets and the surface of the test plate (summit of the bump) was 4.5*d* (diam-eters of the jet). The height of the bump is 3 mm. The idea of the heat transfer enhancement by shape surface modification is to elongate the high stress region, created under impinging jet, along the wall camber, namely along the bump. The scheme of the flow pattern during the heat transfer experiment on the bump and schematic geometry of the bump in the ex-perimental investigations are presented in Fig. 7. According to its shape the bump will be called ‘mild’.

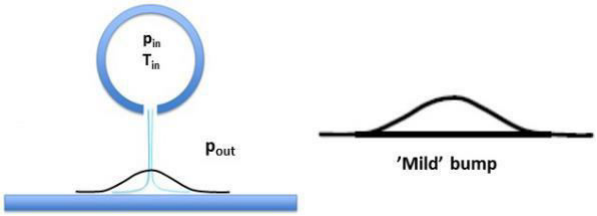

Figure 7: Schematic view of the flow over the bump and bump shape.

4 Temperature field determination

The temperature distribution is calculated from the data like depicted in Fig. 6 by using the calibration curves of the liquid crystals. An exem-plary set of calibration points is depicted in Fig. 8. These points indicate the relation of TLC (liquid crystal thermography) colour (in terms of red, green and blue component value) and the temperature. Red (R), green (G) and blue (B) components are the values of analog-to-digital (camera) con-verter describing the intensity of corresponding light band intensity (non-dimensional value). They are acquired in the process of in-situ calibration, which is done by heating the foil to a set of temperatures (domain in Fig. 8, measured with a K type thermocouple during the experiment). When the desired temperature is achieved, a photograph of the region is taken and the values of colour components are extracted. Based on this set of discrete points, the continuous calibration curves are interpolated (like in Fig. 9).

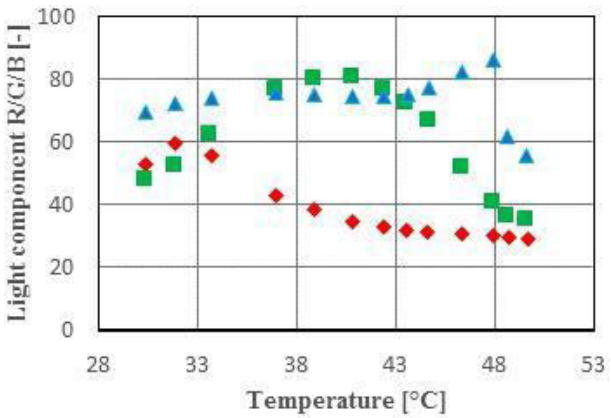

Figure 8: TLC calibration points: red (diamond), green (square), and blue (triangle) light components with respect to the temperature.

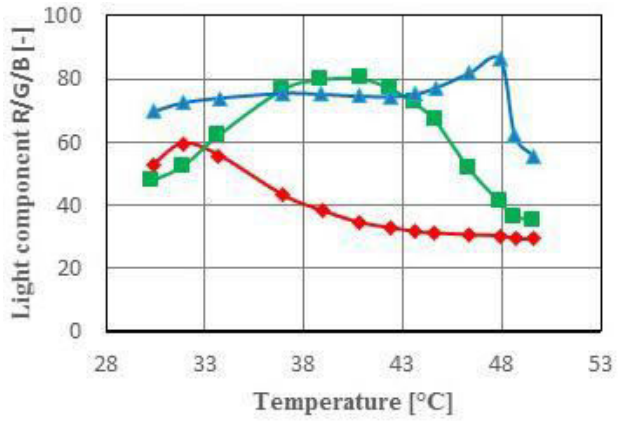

Figure 9: TLC calibration curves: red (diamond), green (square), and blue (triangle) lightcomponents with respect to the temperature.

The interpolation is conducted with the temperature step of approximately 0.2°C, which is the resolution of recovering the temperature values from experimental data that we have. Due to the complex geometry of the bump and varying the camera position between the taken frames, it was impossible to have the same light conditions on the whole plate. An exemplary image showing this issue is depicted in Fig. 10. In the centre of the image one can see brighter region.

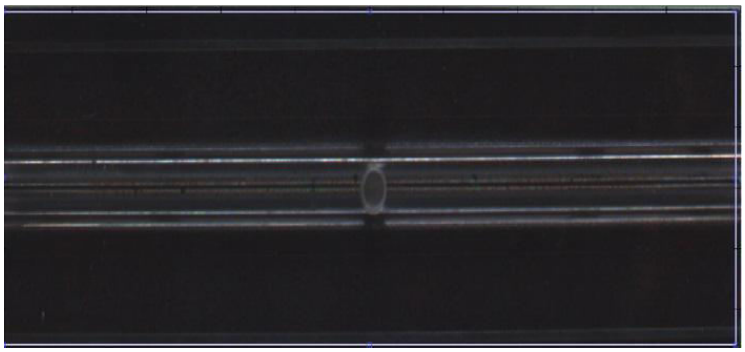

Figure 10: Calibration photograph with non-uniform light conditions.

The whole region of interest is divided to subregions of a desired size, and then an individual calibration for every region is calculated. The size of the regions in calibration used for obtaining HTC is 2 ×2 pixels. The regions in

Fig. 11 are of exaggerated size (50×50 pixels) only for illustrative purposes. Figure 12 illustrates the significance of the differences between calibrations in various subregions of the image.

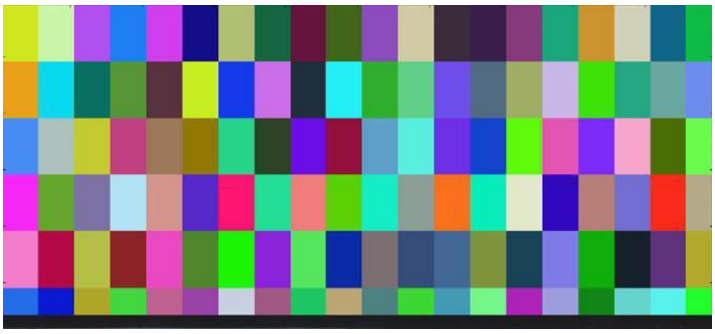

Figure 11: Subregions (50 × 50 pixels) of calibration.

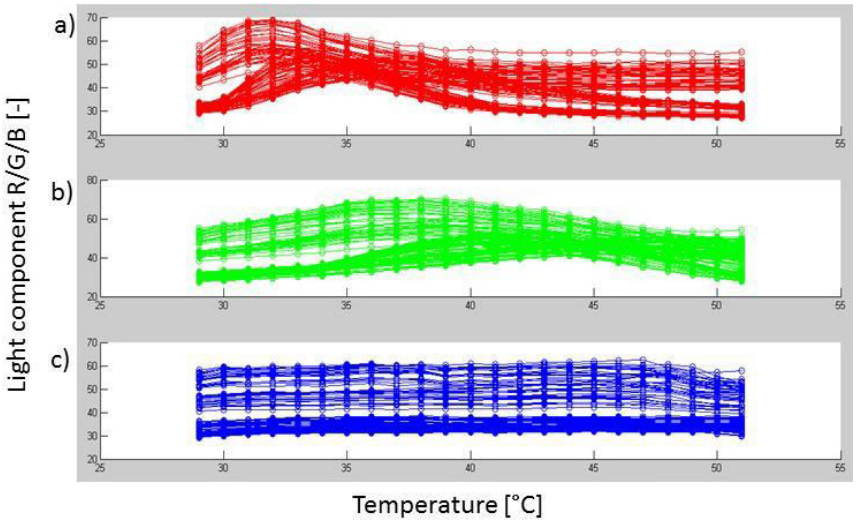

Figure 12: Comparison of a) red, b) green, and c) blue light components calibration curves with respect to the temperature.

A Matlab application [20] for determining temperature from the local colour, exploiting correct set of calibration curves in every point, has been devel-oped. An exemplary map of temperature calculated from a photograph is shown in Fig. 13.

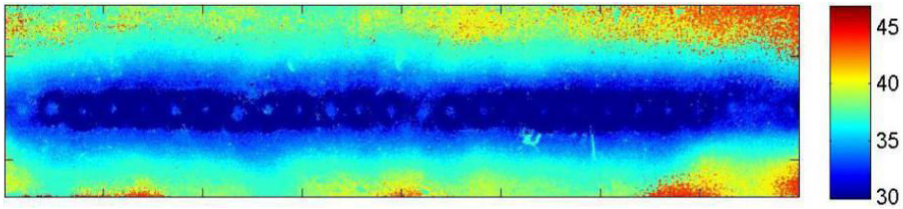

Figure 13: Map of temperature calculated from a photograph.

5 Heat transfer coefficient calculations

Further, when the temperature field during the experiment is found, the heat transfer coefficient is calculated from

$$\text{HTC} = \frac{q_{conv}}{\Delta T}, \tag{1}$$

where q_{conv} represents the heat flux exchanged by convection between the tested surface and the mainstream flow, $\Delta T = T_W - T_{amb}$ is the temperature difference between the discrete point on the wall (measured by means of LC) and the jet temperature, the same as the ambient air. To correctly evaluate q_{conv}, the conductive heat losses across the PMMA surface (q_{cond}) must be accounted for. To calculate that following 1D approach, the q_{conv} is expressed by

$$q_{conv} = q_{joule} - q_{cond} = q_{joule} - \frac{k}{s}(T_W - T_{amb}), \tag{2}$$

where q_{joule} is the electric power of the heater foil, s represents the tested surface thickness and k is the thermal conductivity of the PMMA.

The heat flux value is calculated as the electric power of the heater foil (q_{joule}) reduced by a factor resulting from the conduction of heat from the foil to the wall. Equation (1) stands in every point of the domain, *i.e.* the set of equations for the whole surface is uncoupled and can be solved in every point (pixel) of the investigated temperature field independently, yielding a distribution of HTC over the surface. The 1D approach used in the flat plate geometry for the HTC calculations was used in the curved surface case due to the fact that the bump size was relatively small compared to the plate dimensions. Nevertheless, a more complex model should be used if the size of the bump is significant and curvature of the surface does not allow to assume the 1D case.

6 Heat transfer measurements – results

The comparison of normalized HTC distribution (HTC/HTCmax.) aver-aged along the channel for flow cases at Re = 2500 is shown in Fig. 14. This distribution shows that the HTC peak for a mild bump (solid line) is about 30% higher in relation to the reference flow case (flat plate, black line), also the region of a higher level of heat transfer from jets centre line spreads much wider. The comparison of normalized HTC distribution av-eraged along the channel for flow cases at Re = 4000 is shown in Fig. 15.

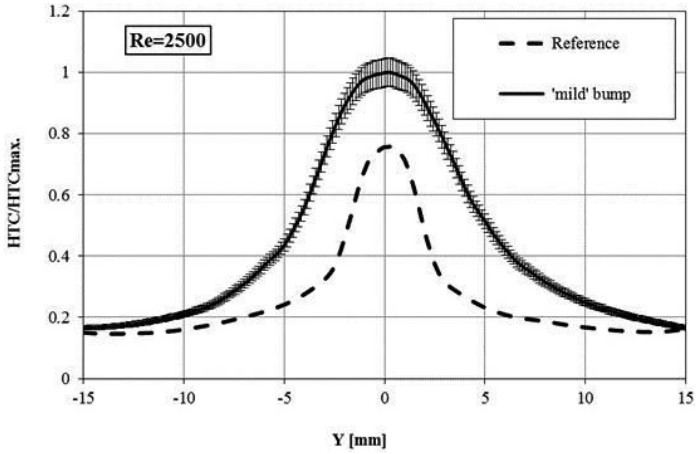

Figure 14: Normalized HTC distribution for Re = 2500.

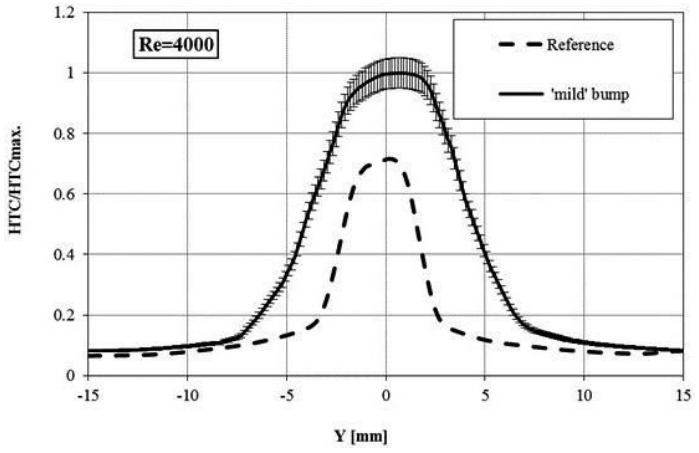

Figure 15: Normalized HTC distribution for Re = 4000.

The difference in the HTC peak for a mild bump for Re = 4000 case is about 35% higher compared to the reference case. Again, like it was stated for Re = 2500 case, the region of higher level of heat transfer spreads much wider from the jets centre line. Maximum errors of the HTC measurements for ‘mild’ bumps were 5.27% and 12.53% for Re = 2500 and Re = 4000, respectively. Maximum errors of the HTC measurements for reference cases were 4.56% and 9.33% for Re = 2500 and Re = 4000, respectively. For the sake of figures clarity only error bars for mild bumps are presented.

7 Conclusions

Experimental investigations were carried out to study the heat transfer dis-tribution between the impinging jets from a long round pipe and a plate with different surface configurations. The main objective of the performed research was to investigate the influence of the presence and shape of the bump on the distribution of heat transfer coefficient under the row of im-pinging jets. The results of ‘mild’ bump shape were compared against the flat plate results (reference case) in terms of heat transfer efficiency. Reynolds number based on the jet orifice exit conditions was varied be-tween 2500 and 4000. For such Reynolds numbers the flow velocity in jets was particularly very high, changing from the Mach number of 0.56 to 0.77. The following conclusions can be drawn from the presented experimental investigations:

1. Based on the preliminary measurements of heat exchange on the flat plate, surface modification has been introduced – ‘mild’ bump. Com-pared to the reference case, modified surface HTC measurements required use of mirrors to capture the heat exchange on the bump slopes. A Matlab code for determining the temperature field from the liquid crystal colour has been developed and used for heat transfer coefficient calculations.

2. To ensure the adjoining of liquid crystal foil and surface with a bump, a system of ducts and holes around the liquid crystal foil has been introduced to remove the air by air suction system. A lower pres-sure level in the suction system in relation to the test section has been kept by the vacuum pumps operating continuously during the measurement campaign.

3. Higher values of mean heat transfer coefficient were observed for all flow cases with a bump in relation to the reference flow. A proper wall modification can cause an increase of averaged heat transfer coefficient in the range of 30–35%, the exact value depends on the flow case.
4. The high jet velocity can have an influence on jet impingement heat transfer. In certain cases the Reynolds number is not enough to describe the mean heat transfer coefficient on the impinged surface. The high flow velocity tends to improve heat exchange on the surface. Compressible effects should be taken into account with high velocity impinging jets.
5. As the geometry inside the external cooling system of low pressure gas turbine casing is very complex, the accuracy of manufacturing and assembling can play a crucial role in the heat exchange between the jets and cooled surfaces especially in the areas where the surfaces are not flat. Shift of the 'sharp' edge from the cooling jet centre line can reduce the heat exchange.

Acknowledgements This work was supported by sectoral project INNOLOT, the Coopernik project "Cooperative Research for Next Generation High Efficiency Low Pressure Turbine" – INNOLOT/I/11/NCBR/2014.

Received 29 January 2021

References

[1] Gołdasz A., Malinowski Z.: *Identification of the Heat Transfer Coefficient at the Charge Surface Heated on the Chamber Furnace*. Arch. Metall. Mater. **62**(2017), 2, 509–513.

[2] Taler D., Gradziel S., Taler J.: *Measurement of heat flux density and heat transfer coefficient.* Arch. Thermodyn. **31**(2010), 3, 3–18.

[3] Livingood J.N.B., Hrycak P.: *Impingement heat transfer from turbulent air jets to flat plates: A literature survey*. NASA Tech. Mem. – TM X-2778, E-7298, ID: 19730016200, RTOP 501-24 (1973).

[4] Martin H.: *Heat and mass transfer between impinging gas jets and solid surfaces*. Adv. Heat Transf. **13**(1977), 1–60.

[5] Downs S.J., James E.H.: *Jet impingement heat transfer – A literature survey*. In: Proc. ASME, AIChE, ANS, 24th Nat. Heat Transfer Conf. Exhib., Pittsburgh,. 1987, ASME pap. 87-HT-35.

[6] Jambunathan K., Lai E., Moss M.A., Button B.L.: *A review of heat transfer data for single circular jet impingement*. Int. J. Heat Fluid Fl. **13**(1992), 2, 106–115.
[7] Ashforth-Frost S., Jambunathan K., Whitney C.F.: *Velocity and turbulence characteristics of a semiconfined orthogonally impinging slot jet*. Exp. Therm. Fluid Sci. **14**(1997), 1, 60–67.
[8] Hoogendoorn C.J.: *The effect of turbulence on heat transfer at a stagnation point*. Int. J. Heat and Mass Tran. **20**(1977), 12, 1333–1338.
[9] Zhe J., Modi V.: *Near wall measurements for a turbulent impinging slot jet*. J. Fluid. Eng.-T. ASME **123**(2001), 1, 112–120.
[10] Brevet P., Dorignac E., Vullierme J.J.: *Mach number effect on jet impinge-ment heat transfer*. Ann. N.Y. Acad. Sci. **934**(2001), 1, 409–416.
[11] Koopman R.N.N., Sparrow E.M.M.: *Local and average transfer coefficients due to an impinging row of jets*. Int. J. Heat Mass Tran. **19**(1976), 6, 673–683.
[12] Kercher D., Tabakoff W.: *Heat transfer by a square array of round air jets impinging perpendicular to flat surface including the effect of spent air*. J. Eng. Power-T. ASME **92**(1970), 1, 73–82.
[13] Florschuetz L., Truman C., Metzger D.: *Streamwise flow and heat transfer distributions for jet array impingement with crossflow*. J. Heat Transf.-T. ASME **103**(1981), 2, 337–342.
[14] Behbahani A., Goldstein R.: *Local heat transfer to staggered arrays of impinging circular air jets*. ASME J. Eng. Power-T. ASME **105**(1983), 2, 354–360.
[15] Goodro M., Park J., Ligrani P., Fox M., Moon H.: *Effects of Mach number and Reynolds number on jet array impingement heat transfer*. Int. J. Heat Mass Tran. **50**(2007), 1, 367–380.
[16] Andreini A., Da Soghe R., Facchini B., Miauolo F., Tarchi L.: *Experimental and numerical analysis of multiple impingement jet arrays for an active clearance control system*. In: Proc. ASME Turbo Expo 2012, Vol. 4, June 11–15, 2012, Copen-hagen, GT2012-68791, 287–299.
[17] Ryfa A., Rojczyk M., Adamczyk W.: *On influence of selected parameters on the spatial distribution of the heat transfer coefficient for an array of air jets*. Appl. Therm. Eng. **146**(2019), 21–29.
[18] Shukla A.K. and Dewan A.: *Flow and thermal characteristics of jet impingement: comprehensive review*. Int. J. Heat Technol. **35**(2017), 1, 153–166.
[19] Kurowski M., Szwaba R., Telega J., Flaszynski P., Tejero F., Doerffer P.: *Wall distance effect on heat transfer at high flow velocity*. Aircr. Eng. Aerosp. Tec. **91**(2019), 9, 1180–1186.
[20] https://www.mathworks.com/products/matlab.html (accessed 3 Nov. 2020).